Pressure measurement by low coherence speckle interferometry membrane shaping with tunable diode lasers

Marcelo Tadao Saita
Instituto de Pesquisas Tecnológicas
São Paulo, Brasil
marcelo.saita@hotmail.com

Eduardo Acedo Barbosa
Unidade de Pós-Graduação, Extensão e Pesquisa,
CEETEPS,
São Paulo, Brasil
ebarbosa@fatecsp.br

Francisco Tadeu Degasperi
Unidade de Pós-Graduação, Extensão e Pesquisa,
CEETEPS,
São Paulo, Brasil
ftd@fatecsp.br

Niklaus Ursus Wetter
Centro de Lasers e Aplicações
Instituto de Pesquisas Energéticas e Nucleares
São Paulo, Brasil
nuwetter.ipen@gmail.com

***Abstract*— Non-contact evaluation of object deformation is of great importance in several industrial and scientific processes. In this work the demonstrate that low-coherence digital speckle pattern interferometry can be employed for pressure measurement by the analysis of a 0.4-mm thickness, 55-mm diameter circular aluminum membrane submitted to a pressure differential ranging from 0 to 90 kPa. The membrane deformation was measured with a tunable red diode laser emitting simultaneously two wavelengths. The resulting speckle image of the membrane appeared covered with interference fringes which correspond to the contour lines of the studied surface. By means of conventional fringe pattern evaluation methods like 4-stepping and unwrapping methods the membrane deformation was determined. The experimental results were compared with the ones obtained by a numerical algorithm.**

***Keywords*— Speckle, Interferometry, Deformation, Pressure.)**

I. INTRODUCTION

Along the years the use of interferometry for pressure measurement was proposed by several authors [1-6]. Those techniques basically measure the deformation of membranes or diaphragms in the range from hundreds of micrometers up to several millimeters. In this framework we propose the deformation measurement of a membrane submitted to a pressure differential by low coherence speckle interferometry. For this purpose the interferometer is illuminated by a tunable diode laser, which allows selecting the most suitable emission parameters according to a required sensitivity [7]. In addition, low coherence techniques do not require very severe stability conditions, if compared with other conventional interferometry methods [8].

II. THEORY

A. Low coherence speckle interferometry

Objects with rough surfaces illuminated simultaneously by two laser beams with slightly different wavelengths λ_1 and λ_2 may generate an object image modulated by low spatial frequency fringes in a DSPI (Digital Speckle Pattern Interferometry) setup [9]. Each contour fringe of the resulting interferogram corresponds to a plane of constant elevation. The distance between adjacent planes is closely related to the synthetic wavelength .

The light intensity resulting from the interference of the studied object wave and the reference wave is recorded onto a CCD target. The background noise due to the reference beam intensity is removed with the help of the subtraction method [9], so that the contour fringe pattern intensity is given by [10]

$$I(x,y) = I_0 \cos^2\left[\frac{\pi(\Gamma_S(x,y) - \Gamma_R)}{\lambda_S}\right] \qquad (1)$$

Equation (1) above was obtained considering that each laser mode has the same intensity I_0. $\Gamma_S(x,y)$ is the optical path of the object beam through a point (x,y) on the object surface and Γ_R is the reference beam path.

B. External cavity diode laser

By properly selecting wavelengths λ_1 and λ_2 the synthetic wavelength value can be conveniently set according to the surface dimensions and geometry. We used the Littman-Metcalf (LM) feedback technique whose setup is shown in figure 1. This technique is based on a controlled feedback by an external cavity with a diffraction grating for emission wavelength selection and modes stabilization [11, 12].

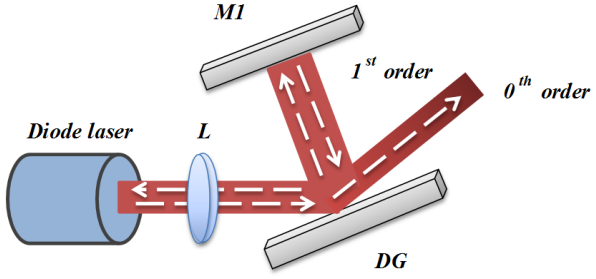

Figure 1. Littman-Metcalf (LM) optical setup: L, lens; DG, diffraction grating; M1, mirror.

978-1-5386-6702-6/18/$31.00 ©2018 IEEE

The main component of the LM setup is the diffraction grating. As shown in figure 1, the 0th-order diffracted beam is used to illuminate the interferometer. The mode selection is made as the -1 order beam is reflected by the properly adjusted mirror M1 back to the grating and consequently to the laser. Only the modes selected by M1 are reinforced inside the laser diode and have enough gain to oscillate. Thus, the spectral content of the laser inciding into the speckle interferometer is directly determined by the LM setup.

III. Experiments

In the proposed method, the pressure was determined by evaluating the deformation undergone by a diaphragm (or membrane) submitted to a pressure differential. Several pressure values were applied on the diaphragm and their respective deformation values were measured. By using software COMSOL Multiphysics an experimental relation between measured deformation and pressure was determined.

Figure 2 shows in detail the aluminum membrane holder. At the left illuminated face there is atmospheric air, while at the internal right side the pressure to be measured. In this configuration the device measures "gauge pressure" where positive values represents pressures above the atmospheric pressure and negative values represents pressures below the atmospheric pressure [13]. Figure 3 shows schematically the vacuum pump system.

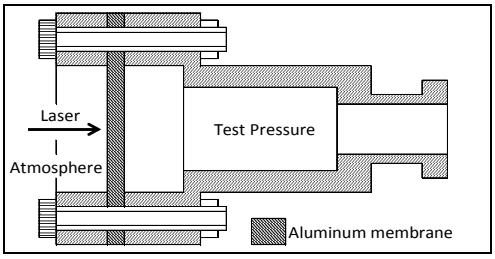

Fig. 1 – Membrane assembly

The vacuum system consists of a mechanical vane vacuum pump, a valve (valve 2) to isolate the vacuum pump from the membrane housing, a needle valve (valve 1) to adjust pressure, and standard pumping.

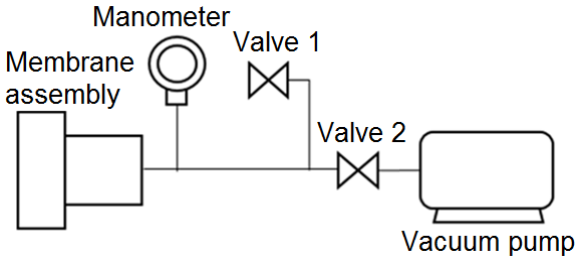

Fig. 3. Vacuum pump system

In the speckle interferometer the beam leaves de LM arrangement and is divided into reference and object arms at beam splitter BS1. In the object arm, the beam is collimated by lenses L1 and L2, hits the object after passing through beam splitter BS2. The light scattered by the diffusive membrane passes through mirror M3 and beam splitter BS3, and the membrane image is formed at the 15-µm pixel size CCD camera by lens L5.

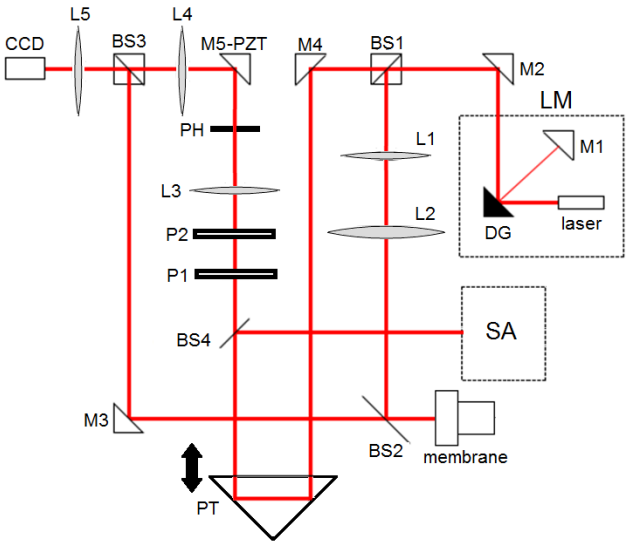

Figure 4. Optical setup

At the left BS2 side the reference beam passes through a 90-degree prism translator PT, which can be translated (see fig. 4) with the help of a micrometric screw, not shown in figure 4, in order to perform the 4-stepping procedure [9]. After being reflected by PT, the beam passes through polarizers P1 and P2 for intensity selection – P2 transmission axis is kept vertical to the table top while P1 can be rotated in order to achieve the best object beam to reference beam intensity ratio - and pinhole PH for beam spatial filtering. Lenses L4 and L5 collimate the reference beam to interfere with the object beam at the CCD target. Mirror M5-PZT is supported by a piezoelectric ceramic vibrating at 5 Hz in order to perform the subtraction method for fringe visibility enhancement [9]. At beam splitter BS4 the beam is partially deviated to allow real time spectrum monitoring at the home-made spectrum analyzer SA.

IV. Results

A. Fringe evaluation

Figure 5a shows the resulting phase map after applying the 4-stepping procedure in which a complete set of four sequentially π/2-shifted interferograms is acquired for a given membrane deformation. The concentric circular fringes in those frames show clearly that the maximum deformation was achieved at the central part of the membrane. Figure 5b in turn shows the unwrapped phase of the membrane. The darker the gray level, the lower the vertical displacement of a point on the membrane. The figure shows that the darkest central region of the membrane corresponds to its largest deformation. For each pressure differential applied to membrane, a set of four frames, a phase map and an unwrapped phase [14] like the ones of figure 5 were obtained. After converting the gray levels of the unwrapped phase into height coordinate values, one obtains a deformation map of the surface.

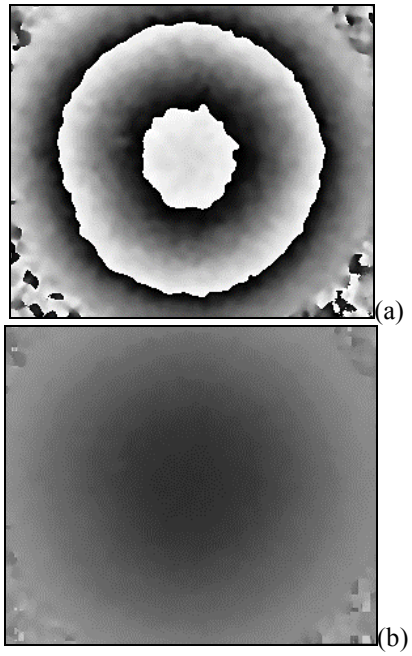

Fig. 5. a – Phase map; b – unwrapped phase.

B. *Deformation measurement*

Table 1 shows the relevant material and dimensional properties of the aluminum alloy used in the numerical calculations. The average membrane thickness is 423 ± 3 µm and its diameter is 55.00 ± 0.04 mm.

Table 1. Mechanical properties of the aluminum alloy [14]

Material	Elasticity modulus	Poisson Coefficient	Thermal expansion
Aluminium alloy	72 GPa	0,33	23,5 µ/°C

Figure 6 shows the experimental values of maximum deformation undergone by the membrane and compare them with values numerically obtained by the software COMSOL Multiphysics (version 5.1). Each interferometric value was obtained after a series of three measurements, from which the error bars were obtained. The measurement hysteresis values are slightly below the uncertainty ones. For each pressure value, the input dada for the numerical calculation were obtained from table 1.

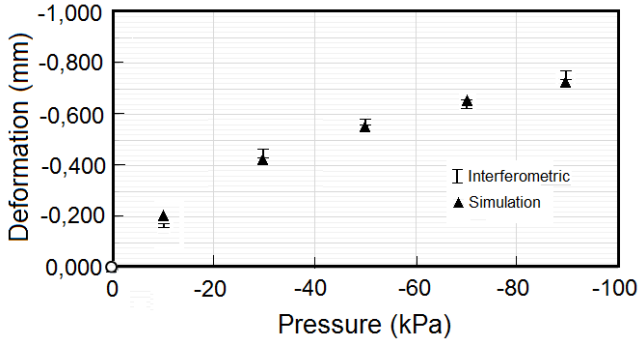

Fig. 6. Maximum deformation of the membrane submitted to the pressure differential. Vertical bars, experimental results obtained from low coherence speckle interferometry; triangles, numerical results.

CONCLUSION

The membrane deformation was successfully measured by the proposed optical arrangement and the experimental results were compared with a numerical simulation. The experimental results presented very small and no systematic deviations from the numerical results. The errors could be mainly attributed to fluctuations in the laser emission due temperature variations or to instabilities in the drive current. The authors are currently working on an uncertainty model for the measurements to improve the analysis of the results.

ACKNOWLEDGMENT

The preferred spelling of the word “acknowledgment” in America is without an “e” after the “g”. Avoid the stilted expression “one of us (R. B. G.) thanks ...”. Instead, try “R. B. G. thanks...”. Put sponsor acknowledgments in the unnumbered footnote on the first page.

REFERENCES

[1] K. Benaissa, A. Nathan, “IC compatible optomechanical pressure sensors using Mach-Zehnder interferometry” IEEE Trans. on Electron. Devices, vol. 43, pp. 1571-1582, September 1996.

[2] J. M. Huntley, H. O. Saldner, “Multi-channel pressure sensor using speckle interferometry” Opt. Las Engng. Vol. 23, pp. 263-275, 1995.

[3] M. Li; M. Wang, H. Li, “Optical MEMS pressure sensor based on Fabry-Perot interferometry,” Opt. Express, vol. 14, pp.1497-1504, February 2006.

[4] C Pang, H Bae, A Gupta, K Bryden, M Yu, “MEMS Fabry-Perot sensor interrogated by optical system-on-a-chip for simultaneous pressure and temperature sensing,” Opt. Express, vol. 21, pp. 21829-21839, July 2013.

[5] F. J. Torres, “Application of digital holographic interferometry to pressure measurements of symmetric, supercritical, and circulation control airfoils in transonic flow fields” Proceedings of High speed photography, videography, and photonics IV; 1986. International Society for Optics and Photonics.

[6] K. Totsu, Y. Haga, M. Esashi, “Ultra-miniature fiber-optic pressure sensor using white light interferometry”, Journal of Micromechanics and Microengineering, vol. 15, October 2004.

[7] D.M. da Silva, E.A. Barbosa, N.U.Wetter, “Real-time contour fringes obtained with a variable synthetic wavelength from a single diode laser” Applied Physics B, vol. 118, pp. 159-166, Dec. 2014.

[8] D. Francis D. Masiyano, J. Hodgkinson, R. P. Tatam. “A mechanically stable laser diode speckle interferometer for surface contouring and displacement measurement,” Measurement Science and Technology, vol. 26 pp. 055402, April 2015.

[9] E. Hack, B. Frei, R. Kästle, U. Sennhauser, “Additive-subtractive two-wavelength ESPI contouring by using a synthetic wavelength phase shift”, Appl. Opt., vol 37, pp. 2591–2597, 1998.

[10] E.A. Barbosa, A.C.L. Lino, “Multiwavelength electronic speckle pattern interferometry for surface shape measurement,” Appl. Opt. vol. 46, pp. 2624-2631,2007;

[11] M.G. Littman, H.J. Metcalf, “Spectrally narrow pulsed dye laser without beam expander,” Appl. Opt., vol 17, pp. 2224-2227, 1978.

[12] K. Liu; M. G. Littman, “Novel geometry for single-mode scanning of tunable lasers,” Opt. Lett. vol. 6, pp. 117-118, 1981.

[13] Cusco, L. et al. Guide to the Measurement of Pressure and Vacuum. The Institute of Measurement and Control, London, 1998.

[14] B. Gutmann , H. Weber, “Phase unwrapping with the branch-cut method: role of phase-field direction”, Appl Opt. vol. 39, pp. 4802-4816, 2000.